AJR FOCUS ON:

# Translational Optical Imaging

Adrian Taruttis[1]
Vasilis Ntziachristos

**OBJECTIVE.** Optical imaging is experiencing significant technologic advances. Simultaneously, an array of specific optical imaging agents has brought new capabilities to biomedical research and is edging toward clinical use. We review progress in the translation of macroscopic optical imaging—including fluorescence-guided surgery and endoscopy, intravascular fluorescence imaging, diffuse fluorescence and optical tomography, and multispectral optoacoustics (photoacoustics)—for applications ranging from tumor resection and assessment of atherosclerotic plaques to dermatologic and breast examinations.

**CONCLUSION.** Optical imaging could play a major role in the move from imaging of structure and morphology to the visualization of the individual biologic processes underlying disease and could, therefore, contribute to more accurate diagnostics and improved treatment efficacy.

Several factors motivate the translation of optical imaging techniques. Advanced optical imaging could improve on the limitations of clinical decision making based on visual inspection—for example, decisions made by surgeons in the operating room. Human vision is not suited for seeing under the tissue surface and has difficulties distinguishing small clusters of cells or detecting molecular processes associated with disease. Traditional radiologic modalities including MRI and CT that rely on large devices are often not applicable in situations in which continuous access to the patient is required; again, an operating room is a good example. Instrumentation for optical imaging, on the other hand, is relatively inexpensive, simple, and portable and could be readily disseminated in endoscopic or surgical suites and beyond. Detection is generally highly sensitive: Fluorescence can be detected at subpicomole concentrations, and optoacoustics has a high sensitivity for detecting endogenous chromophores, such as hemoglobin or melanin, and a variety of photoabsorbing nanoparticles [1]. The multispectral capabilities of optical imaging allow multiple different molecules and probes to be concurrently resolved, potentially providing multiplexed information on tissue biomarkers.

The near-infrared (NIR) part of the light spectrum, particularly 650–900 nm, has been extensively considered for in vivo tissue imaging applications because light in this wavelength range typically propagates for several centimeters because of the low absorption of NIR photons by tissue [2]. However, by moving deeper into tissue, the effects of photon scattering become very strong and deteriorate imaging performance even if sufficient penetration is achieved. For typical tissues, light loses its directionality in the depth range of 0.5–1 mm [3]. This characteristic of light restricts high-resolution optical methods, such as multiphoton microscopy, to within these depths. However, tomographic techniques, including optical tomography using diffusive photons, optoacoustic tomography, and hybrid methods, provide meaningful images regardless. In the case of optoacoustics, high-resolution deep tissue imaging is possible.

Visualization of endogenous tissue contrast, such as hemoglobin concentration, oxygenation, and blood vessel structures, can be achieved with relatively few regulatory hurdles, but the significant costs associated with the approval of exogenously administered agents have, to date, limited their clinical translation despite potential benefits. Although there is no optical agent with molecular specificity that has been approved for routine clinical use, exploratory trials have been initiated that, if successful, may lead to an important departure from current optical imaging in clinical practice. In addition, induced tissue autofluorescence approaches have shown advanced clinical potential [4, 5]. Preclinically, a number of optically labeled

**Keywords:** infrared imaging, optical imaging

DOI:10.2214/AJR.11.8431

V. Ntziachristos received support from the ERC Advanced Investigator Award and the German Ministry of Education (BMBF) Innovation in Medicine Award and is an equity holder in iThera Medical GmBH.

Received December 13, 2011; accepted after revision March 12, 2012.

[1]Both authors: Institute for Biological and Medical Imaging, Helmholtz Zentrum München, Ingolstädter Landstrasse 1, 85764 Neuherberg, Germany. Address correspondence to V. Ntziachristos (v.ntziachristos@tum.de).

*AJR* 2012; 199:263–271

0361–803X/12/1992–263

ligands have been confirmed for in vivo imaging in animal models. Typical labels used are small-molecule fluorescent dyes; however, a range of nanoparticles have also been considered for fluorescence and optoacoustic applications (e.g., quantum dots, gold nanorods, or carbon nanotubes). In the case of inorganic nanoparticles, much debate remains about the potential for clinical translation because of toxicity concerns [6]. Other technologies for generating optical contrast include agents that modify an optical parameter on interaction with a biologic target—for example, the activation of quenched fluorescent dyes after molecular modification of the probe by an enzyme, which has been used to visualize protease upregulation in atherosclerotic plaques [7, 8]. The prospect of such agents gaining clinical approval shifts the outlook for translational optical imaging.

In this article, we concentrate on recent optical technologies that have shown potential for clinical use. We discuss the emerging field of fluorescence-guided surgery and the potential of intravascular fluorescence imaging for assessing biomarkers in atherosclerosis. Tomographic techniques that allow imaging deeper in tissue, offering quantitative volumetric optical imaging, are also reviewed. Finally, the clinical potential of optoacoustic (photoacoustic) methods is also discussed; in particular, we discuss multispectral optoacoustic imaging, an emerging modality that offers high-resolution optical imaging through several millimeters to centimeters in tissue.

## Fluorescence Imaging in Surgery and Endoscopy

For centuries, surgeons have relied on their vision and tactile information for distinguishing between tissue types—for example, in differentiating tumors from healthy surrounding tissue. However, human vision provides low contrast: Hemoglobin and tissue scattering dominate the visual appearance. Using fluorescent agents has therefore gained attention for enhancing surgical vision and guiding the surgeon toward identification of sentinel lymph nodes and more accurate tumor delineation. Specialized, highly sensitive camera systems with appropriate illumination to excite the fluorochromes as well as suitable emission filters are required. Several of these systems have been developed and, in general, allow the fluorescence distribution to be displayed in real time over a color or black-and-white video [9–11] (Fig. 1A).

Animal studies have shown the added value of fluorescence guidance during surgery in models of breast cancer [12], ischemic bowel disease [13] (Fig. 1B), and several other applications. In humans, progress has been slowed by the lack of approved specific fluorescent agents. A large body of work has, however, been conducted using indocyanine green (ICG), an approved NIR dye, for surgical guidance in humans; this work started with lymphatic mapping [14–16] and now includes liver cancer enhancement facilitated by accumulation of ICG around tumors as a result of biliary excretion disorders [17]. Endoscopic examination of superficial gastric tumors has been aided by passive accumulation of ICG [18, 19].

The most advanced approaches in terms of clinical trials are those that apply aminolevulinic acid (ALA) to enhance the generation of porphyrin in tumors, which provides visible fluorescence. ALA has been applied for fluorescence cystoscopy and guided resection in patients with bladder cancer [5] and has been reported to improve recurrence rates after 12 months, from 47% with white light to 31% using fluorescence in 145 patients [20], and to achieve a higher rate of carcinoma in situ detection, 87% versus 75% in 174 patients with detectable lesions [21]. The same principle has been applied in neurosurgery to cause malignant gliomas to fluoresce during operations [4] (Fig. 1C). A study of 322 patients reported in 2006 showed a much higher 6-month progression-free survival using fluorescence-guided surgery (41.0% vs 21.1% with only white light) [22]. However, the use of active tumor-targeting agents is widely considered to be a prerequisite for fluorescence-guided surgery to have a broader clinical impact [23]. Recently, the first study using a tumor-targeted fluorescent agent intraoperatively, folate–fluorescein isothiocyanate (folate-FITC), for ovarian cancer patients was reported [24]. The agent was administered IV and targeted the folate receptor–α, which is overexpressed by 90–95% of human epithelial ovarian cancers. The study found that selected representative fluorescence images of peritoneal metastases allowed surgeons to find, on average, 34 tumor spots against seven in regular color images (Figs. 1D and 1E). Although the fluorochrome applied in that study, FITC, emits light in the visible spectrum and does not therefore allow imaging beyond the tissue surface, this breakthrough points to further such studies in the future.

There are limitations involved in fluorescence-guided surgery. In lymphatic mapping, the use of NIR agents such as ICG enables imaging several millimeters below the skin surface; however, the use of radioisotopes provides much greater depth penetration. Additionally, there are concerns about the quantification of fluorescence signals because variations in tissue absorption properties can have an effect on the detected fluorescence intensity, biasing the data sampled toward low-attenuating lesions. The issue of medical accuracy becomes important, in particular, for comparison of data reported in multicenter clinical trials and data submitted to regulatory agencies. Efforts to deal with this issue using correction approaches based on multispectral imaging are a topic of ongoing investigation [11, 25].

Overall, the promise of fluorescence-guided surgery, a fast-growing field of research, is vast: fewer cases with positive tumor margins, improved sensitivity of metastasis detection, more accurate intraoperative assessment of tissue viability, and so on. The technique can similarly bring benefits to endoscopic procedures—for example, in colonoscopy, bronchoscopy, and esophageal imaging.

## Intravascular Fluorescence Imaging

Several imaging techniques can be applied to assess the structure of atherosclerotic plaques, but few are able to depict the molecular aspects of the key biologic processes that lead to complications [26]. NIR fluorescence imaging has the potential to reveal inflammatory and other atherosclerotic biomarkers in vivo. Because affected arteries such as the coronaries or the carotids are generally not accessible to noninvasive optical techniques, optical imaging of atherosclerosis involves optical fiber–based catheter systems (Fig. 2A) comparable to intravascular ultrasound. An initial study in rabbits in 2008 showed the potential of such methods in detecting fluorescence signals originating from a protease-activated agent in inflamed plaques [27]. Although the system implementation used in that study was limited to displaying one-dimensional signals, the data were convincing, showing a 558% greater peak NIR fluorescence signal in plaques compared with control subjects. Further technical developments, coupled with new rabbit studies, have achieved 2D imaging of the arterial wall to show inflammation in plaques and stent-induced injury [28] (Figs. 2B–2D) and have applied optical frequency domain imaging to allow simultaneous microstructural characterization [29] (Fig. 2E).

A limiting factor for intravascular fluorescence imaging remains the lack of clinically approved agents for molecular imaging, although some interest has been shown in studies

reporting ICG uptake in lipid-rich plaques [30]. Overall, the ability to assess the vulnerability of atherosclerotic plaques by visualizing the underlying biologic processes with intravascular fluorescence imaging could be of great value in future clinical diagnostics. Progress in clinical translation of agents for fluorescence-guided surgery could also benefit intravascular imaging and diagnostics for atherosclerosis in general because some biologic processes are of interest in both cases.

## Diffuse Optical and Fluorescence Tomography

To penetrate deeper than surgical, endoscopic, and intravascular imaging, tomographic approaches using fully diffusive photons have been investigated. In this case, the tissue is typically sequentially illuminated at a multitude of surface points, and the diffusive photons that emanate are measured in parallel at various positions (projections). Photon propagation through the tissue of interest is modeled, typically using a solution to the diffusion equation, and appropriate inversion schemes are applied to obtain quantitative images. This general scheme can equally apply to resolving optical attenuation (absorption, scattering) or fluorescence biodistribution.

Early work in the field of macroscopic optical tomography was performed in the domain of breast imaging aimed at cancer diagnosis. By performing concurrent MRI and diffuse optical tomography with ICG injection of breast cancer patients in 2000, it was shown that lesions could be identified by the absorption enhancement provided by the agent [31]. Later work in the same direction added spectroscopic capabilities by multiwavelength illumination, providing maps of hemoglobin oxygenation and other chromophore signatures through the breast [32] (Fig. 3). By this time, information from the MRI volumes was being applied to improve the reconstruction accuracy of the optical images, resulting in true hybrid imaging. A subsequent diffuse optical imaging study of 23 breast cancer patients found a correlation between neoadjuvant chemotherapy response and oxyhemoglobin signatures: A statistically significant increase in oxyhemoglobin on day 1 after the first infusion was found in responding tumors compared with no increase in nonresponding tumors [33]. A separate but similar study of 11 patients found that total tissue hemoglobin as measured by the same method could predict complete compared with partial pathologic response on the basis of decreased values [34]. Further applications of tomographic optical techniques include imaging of rheumatoid arthritis; a recent study reporting results of 99 arthritic patients showed possible sensitivities and specificities of more than 85% using only endogenous absorption contrast [35]. There is also significant interest in the application of diffuse optical tomography to neuroimaging—for example, in the study of functional connectivity for diagnostic purposes in preterm infants [36].

Fluorescent molecular tomography of mice was also developed to volumetrically image fluorescence probes in vivo and provided quantitative 3D imaging of protease activity in tumors [37], macrophage infiltration in myocardial infarction [38], and a range of other targets of interest in biomedical research. More recent efforts have focused on combining fluorescent molecular tomography with modalities such as CT or MRI to provide anatomic reference as well as improved reconstruction accuracy [39–41].

Despite early clinical demonstration of optical tomographic methods, propagation into the clinic has been slow. However, the technologic capabilities are proven, and if combined with optical molecular agents, they may bring new performance in tackling unmet clinical need.

## Multispectral Optoacoustic Imaging

The performance of all purely optical methods is limited by photon scattering, which complicates the accuracy in image formation and degrades spatial resolution in deep tissue. In response, optoacoustic methods have been considered for optical imaging in biomedicine. Optoacoustic imaging is not affected by the photon-scattering barrier: Absorption of light can be resolved by means of ultrasound waves emitted as a result of local thermal expansion at the site of each absorber. In other words, optoacoustic images display optical contrast at ultrasound resolutions. Because ultrasound scatters orders of magnitude less than light in tissue, when clinically relevant ultrasonic frequencies are used, high spatial resolutions can be preserved through millimeters to centimeters of penetration. Optoacoustic spectroscopy and simple imaging have been performed since the late 1970s [42–44]; however, it is only recently that significant attention has been given to optoacoustics as an alternative to current optical imaging methods [45–48]. Implementations commonly combine diffusive illumination with ultrasound detection at multiple positions around the subject, either by mechanical scanning or by detection arrays such as those used in conventional ultrasound imaging (Fig. 4C). This detection parallelism has been exploited to provide high-rate, real-time visualization (e.g., kidney perfusion [49] [Fig. 4A], tumor perfusion [50], or heartbeat [51]) that enables dynamic imaging; the ease of use could be important in many clinical applications. The penetration depth can be traded off against spatial resolution by changing the frequency of the ultrasound detectors, providing high resolution of small, superficial FOVs, or coarser spatial resolution of larger FOVs in deeper tissue.

The utilization of multiple illumination wavelengths in optoacoustic imaging, often referred to as "multispectral optoacoustic tomography" or "MSOT," enables the specific identification of detected absorbers in the tissue by means of their unique spectral signatures. Hemoglobin is a dominant absorber of light in tissue, so it provides a method not only to resolve blood vessels without exogenous labels, but also to characterize the oxygenation saturation inside those vessels because oxyhemoglobin and deoxyhemoglobin display significantly different optical absorption spectra. Such functional imaging has been performed on small animals in a number of studies at scales ranging from the microscopic [52] (Fig. 4B) to penetration depths of several millimeters [50].

Additional endogenous sources of optical absorption are melanin, of much interest in melanoma imaging of primary tumors [53] and metastases [54], and lipids, an important target in the characterization of atherosclerotic plaques [55, 56]. Exogenous agents suitable for optoacoustic imaging should display a sufficiently high optical absorption to be detected inside tissue. These agents range from simple organic dyes, including clinically approved ICG [49, 57], to experimental light-absorbing nanoparticles such as carbon nanotubes [58], gold nanorods [59, 60], and gold nanospheres [61]. In most of these cases, the addition of targeting mechanisms is possible.

Although optoacoustic imaging has to date most commonly been performed on small animals, clinical applications, in particular those involving breast cancer imaging, have been considered since the 1990s [45]. Preliminary investigations, typically performed at a single wavelength, of patients with suspected breast cancer have considered lesion detection based on increased absorption due to tumor vasculature [62, 63]. In addition, handheld systems for noninvasive lymphatic mapping are under development [64]. Intravascular optoacoustic catheters have been tested on arteries ex vivo to capitalize on the ability to detect lipids [55,

56]. Real-time optoacoustic imaging with 3D vascular mapping of the human arm has been reported [65] (Fig. 4D); this modality, if combined with multispectral oxygenation measurements, could be highly valuable in characterization of peripheral vascular disease. At a smaller scale, optoacoustic microscopy has been applied to imaging of cutaneous microvasculature in humans [66], which will surely be extended to studies of suspected melanoma in the near future.

Because optoacoustic imaging is a relatively new modality, it is difficult to assess the clinical impact that it will have. The natural sensitivity to hemoglobin suggests that it will find applications in label-free vascular imaging, whether for assessing functional parameters of tumor vasculature or aspects of cardiovascular disease. This ability to provide meaningful images without the use of exogenous contrast agents could accelerate translation compared with fluorescence imaging methods, where approval for targeted agents is a prerequisite. On the other hand, there is great interest in the development of novel molecular agents specifically for optoacoustic imaging, some of which could ultimately make their way into the clinics.

## Discussion

Optical imaging could expand clinical vision, from views of morphology provided by current radiologic approaches (e.g., CT, MRI) to visualization of the biologic processes underlying disease, and in many cases could conveniently provide images easily relatable to the tissue of interest during surgical or other procedures. There is a large range of potential clinical uses and applications for optical imaging. Compared with past attempts, significant technologic progress has been achieved—both with systems and with engineered contrast media using optical molecular agents—that brings these new concepts closer to practical clinical translation. Fluorescence-guided surgery promises improved outcomes in cancer patients and more accurate judgment of tissue viability during operations. Intravascular optical imaging has shown the potential to probe the underlying biology in inflamed atherosclerotic plaques and stent-induced injury. Applications could expand more generally to endoscopic approaches, including imaging of the gastrointestinal tract [67]. Diffuse optical tomography could provide improved, simpler diagnosis or "theranostics" of breast cancer and diseases of the extremities, such as arthritis. Multispectral optoacoustic tomography promises deep tissue optical imaging at higher resolutions than previously possible and could find application in dermatology, examination of lymph nodes and breasts, and vascular disease. All of these methods stand to benefit from progress in the development of highly specific molecular optical imaging agents that are ubiquitous in biomedical research and are now starting to find experimental clinical use. Overall, optical imaging could play a major role in the move from imaging of structure and morphology to the visualization of the individual biologic processes underlying disease and could, therefore, contribute to more accurate diagnostics and improved treatment efficacy.

## References


1. Ntziachristos V, Razansky D. Molecular imaging by means of multispectral optoacoustic tomography (MSOT). *Chem Rev* 2010; 110:2783–2794
2. Weissleder R, Ntziachristos V. Shedding light onto live molecular targets. *Nat Med* 2003; 9:123–128
3. Ntziachristos V. Going deeper than microscopy: the optical imaging frontier in biology. *Nat Methods* 2010; 7:603–614
4. Stummer W, Stocker S, Wagner S, et al. Intraoperative detection of malignant gliomas by 5-aminolevulinic acid–induced porphyrin fluorescence. *Neurosurgery* 1998; 42:518–525; discussion, 525–526
5. Witjes JA, Douglass J. The role of hexaminolevulinate fluorescence cystoscopy in bladder cancer. *Nat Clin Pract Urol* 2007; 4:542–549
6. Choi HS, Frangioni JV. Nanoparticles for biomedical imaging: fundamentals of clinical translation. *Mol Imaging* 2010; 9:291–310
7. Deguchi JO, Aikawa M, Tung CH, et al. Inflammation in atherosclerosis: visualizing matrix metalloproteinase action in macrophages in vivo. *Circulation* 2006; 114:55–62
8. Wallis de Vries BM, Hillebrands JL, van Dam GM, et al. Images in cardiovascular medicine: multispectral near-infrared fluorescence molecular imaging of matrix metalloproteinases in a human carotid plaque using a matrix-degrading metalloproteinase-sensitive activatable fluorescent probe. *Circulation* 2009; 119:e534–e536
9. Tagaya N, Yamazaki R, Nakagawa A, et al. Intraoperative identification of sentinel lymph nodes by near-infrared fluorescence imaging in patients with breast cancer. *Am J Surg* 2008; 195:850–853
10. Troyan SL, Kianzad V, Gibbs-Strauss SL, et al. The FLARE intraoperative near-infrared fluorescence imaging system: a first-in-human clinical trial in breast cancer sentinel lymph node mapping. *Ann Surg Oncol* 2009; 16:2943–2952
11. Themelis G, Yoo JS, Soh KS, Schulz R, Ntziachristos V. Real-time intraoperative fluorescence imaging system using light-absorption correction. *J Biomed Opt* 2009; 14:064012
12. Themelis G, Harlaar NJ, Kelder W, et al. Enhancing surgical vision by using real-time imaging of αvβ3-integrin targeted near-infrared fluorescent agent. *Ann Surg Oncol* 2011; 18:3506–3513
13. Matsui A, Winer JH, Laurence RG, Frangioni JV. Predicting the survival of experimental ischaemic small bowel using intraoperative near infrared fluorescence angiography. *Br J Surg* 2011; 98: 1725–1734
14. Kitai T, Inomoto T, Miwa M, Shikayama T. Fluorescence navigation with indocyanine green for detecting sentinel lymph nodes in breast cancer. *Breast Cancer* 2005; 12:211–215
15. Crane LM, Themelis G, Arts HJ, et al. Intraoperative near-infrared fluorescence imaging for sentinel lymph node detection in vulvar cancer: first clinical results. *Gynecol Oncol* 2011; 120:291–295
16. Kelder W, Nimura H, Takahashi N, Mitsumori N, van Dam GM, Yanaga K. Sentinel node mapping with indocyanine green (ICG) and infrared ray detection in early gastric cancer: an accurate method that enables a limited lymphadenectomy. *Eur J Surg Oncol* 2010; 36:552–558
17. Ishizawa T, Fukushima N, Shibahara J, et al. Real-time identification of liver cancers by using indocyanine green fluorescent imaging. *Cancer* 2009; 115:2491–2504
18. Mataki N, Nagao S, Kawaguchi A, et al. Clinical usefulness of a new infrared videoendoscope system for diagnosis of early stage gastric cancer. *Gastrointest Endosc* 2003; 57:336–342
19. Kimura T, Muguruma N, Ito S, et al. Infrared fluorescence endoscopy for the diagnosis of superficial gastric tumors. *Gastrointest Endosc* 2007; 66:37–43
20. Hermann GG, Mogensen K, Carlsson S, Marcussen N, Duun S. Fluorescence-guided transurethral resection of bladder tumours reduces bladder tumour recurrence due to less residual tumour tissue in Ta/T1 patients: a randomized two-centre study. *BJU Int* 2011; 108:E297–E303
21. Lerner SP, Liu H, Wu MF, Thomas YK, Witjes JA. Fluorescence and white light cystoscopy for detection of carcinoma in situ of the urinary bladder. *Urol Oncol* 2011 Mar 9 [Epub ahead of print]
22. Stummer W, Pichlmeier U, Meinel T, Wiestler OD, Zanella F, Reulen HJ. Fluorescence-guided surgery with 5-aminolevulinic acid for resection of malignant glioma: a randomised controlled multicentre phase III trial. *Lancet Oncol* 2006; 7:392–401
23. Schaafsma BE, Mieog JS, Hutteman M, et al. The clinical use of indocyanine green as a near-infrared fluorescent contrast agent for image-guided oncologic surgery. *J Surg Oncol* 2011; 104:323–332
24. van Dam GM, Themelis G, Crane LM, et al. Intraoperative tumor-specific fluorescence imaging in ovarian cancer by folate receptor–α targeting: first in-human results. *Nat Med* 2011; 17:1315–1319
25. Bogaards A, Sterenborg HJ, Trachtenberg J, Wilson BC, Lilge L. In vivo quantification of fluores-

cent molecular markers in real-time by ratio imaging for diagnostic screening and image-guided surgery. *Lasers Surg Med* 2007; 39:605–613

26. Sanz J, Fayad ZA. Imaging of atherosclerotic cardiovascular disease. *Nature* 2008; 451:953–957
27. Jaffer FA, Vinegoni C, John MC, et al. Real-time catheter molecular sensing of inflammation in proteolytically active atherosclerosis. *Circulation* 2008; 118:1802–1809
28. Jaffer FA, Calfon MA, Rosenthal A, et al. Two-dimensional intravascular near-infrared fluorescence molecular imaging of inflammation in atherosclerosis and stent-induced vascular injury. *J Am Coll Cardiol* 2011; 57:2516–2526
29. Yoo H, Kim JW, Shishkov M, et al. Intra-arterial catheter for simultaneous microstructural and molecular imaging in vivo. *Nat Med* 2011; 17:1680–1684
30. Vinegoni C, Botnaru I, Aikawa E, et al. Indocyanine green enables near-infrared fluorescence imaging of lipid-rich, inflamed atherosclerotic plaques. *Sci Transl Med* 2011; 3:84ra45
31. Ntziachristos V, Yodh AG, Schnall M, Chance B. Concurrent MRI and diffuse optical tomography of breast after indocyanine green enhancement. *Proc Natl Acad Sci USA* 2000; 97:2767–2772
32. Brooksby B, Pogue BW, Jiang S, et al. Imaging breast adipose and fibroglandular tissue molecular signatures by using hybrid MRI-guided near-infrared spectral tomography. *Proc Natl Acad Sci USA* 2006; 103:8828–8833
33. Roblyer D, Ueda S, Cerussi A, et al. Optical imaging of breast cancer oxyhemoglobin flare correlates with neoadjuvant chemotherapy response one day after starting treatment. *Proc Natl Acad Sci USA* 2011; 108:14,626–14,631
34. Pakalniskis MG, Wells WA, Schwab MC, et al. Tumor angiogenesis change estimated by using diffuse optical spectroscopic tomography: demonstrated correlation in women undergoing neoadjuvant chemotherapy for invasive breast cancer? *Radiology* 2011; 259:365–374
35. Hielscher AH, Kim HK, Montejo LD, et al. Frequency-domain optical tomographic imaging of arthritic finger joints. *IEEE Trans Med Imaging* 2011; 30:1725–1736
36. White BR, Liao SM, Ferradal SL, Inder TE, Culver JP. Bedside optical imaging of occipital resting-state functional connectivity in neonates. *Neuroimage* 2012; 59:2529–2538
37. Ntziachristos V, Tung CH, Bremer C, Weissleder R. Fluorescence molecular tomography resolves protease activity in vivo. *Nat Med* 2002; 8:757–761
38. Sosnovik DE, Nahrendorf M, Deliolanis N, et al. Fluorescence tomography and magnetic resonance imaging of myocardial macrophage infiltration in infarcted myocardium in vivo. *Circulation* 2007; 115:1384–1391
39. Hyde D, de Kleine R, MacLaurin SA, et al. Hybrid FMT-CT imaging of amyloid-beta plaques in a murine Alzheimer's disease model. *Neuroimage* 2009; 44:1304–1311
40. Schulz RB, Ale A, Sarantopoulos A, et al. Hybrid system for simultaneous fluorescence and x-ray computed tomography. *IEEE Trans Med Imaging* 2010; 29:465–473
41. Ale A, Schulz RB, Sarantopoulos A, Ntziachristos V. Imaging performance of a hybrid x-ray computed tomography-fluorescence molecular tomography system using priors. *Med Phys* 2010; 37:1976–1986
42. Rosencwaig A. Photoacoustic spectroscopy. *Annu Rev Biophys Bioeng* 1980; 9:31–54
43. Busse G. Imaging with the optoacoustic effect. *Opt Laser Technol* 1980; 12:149–154
44. Bowen T. Radiation-induced thermoacoustic soft tissue imaging. In: McAvoy BR, ed. *1981 Ultrasonics Symposium Proceedings*. Piscataway, NJ: IEEE, 1981:817–822
45. Esenaliev RO, Karabutov AA, Oraevsky AA. Sensitivity of laser opto-acoustic imaging in detection of small deeply embedded tumors. *IEEE Journal of Selected Topics in Quantum Electronics* 1999; 5:981–988
46. Kruger RA, Kiser WL, Reinecke DR, Kruger GA, Miller KD. Thermoacoustic molecular imaging of small animals. *Mol Imaging* 2003; 2:113–123
47. Wang X, Pang Y, Ku G, Xie X, Stoica G, Wang LV. Noninvasive laser-induced photoacoustic tomography for structural and functional in vivo imaging of the brain. *Nat Biotechnol* 2003; 21:803–806
48. Razansky D, Distel M, Vinegoni C, et al. Multispectral opto-acoustic tomography of deep-seated fluorescent proteins in vivo. *Nat Photonics* 2009; 3:412–417
49. Buehler A, Herzog E, Razansky D, Ntziachristos V. Video rate optoacoustic tomography of mouse kidney perfusion. *Opt Lett* 2010; 35:2475–2477
50. Herzog E, Taruttis A, Beziere N, Luttich AA, Razansky D, Ntziachristos V. Optical imaging of cancer heterogeneity by means of multispectral optoacoustic tomography (MSOT). *Radiology* 2012; 263:461–468
51. Taruttis A, Shi J, Razansky D, Ntziachristos V. Motion clustering for deblurring multispectral optoacoustic tomography images of the mouse heart. *J Biomed Opt* (in press)
52. Zhang HF, Maslov K, Stoica G, Wang LV. Functional photoacoustic microscopy for high-resolution and noninvasive in vivo imaging. *Nat Biotechnol* 2006; 24:848–851
53. Oh JT, Li ML, Zhang HF, Maslov K, Stoica G, Wang LV. Three-dimensional imaging of skin melanoma in vivo by dual-wavelength photoacoustic microscopy. *J Biomed Opt* 2006; 11:034032
54. Jose J, Grootendorst DJ, Vijn TW, et al. Initial results of imaging melanoma metastasis in resected human lymph nodes using photoacoustic computed tomography. *J Biomed Opt* 2011; 16:096021
55. Jansen K, Van der Steen AFW, van Beusekom HMM, Oosterhuis JW, van Soest G. Intravascular photoacoustic imaging of human coronary atherosclerosis. *Opt Lett* 2011; 36:597–599
56. Sethuraman S, Amirian JH, Litovsky SH, Smalling RW, Emelianov SY. Spectroscopic intravascular photoacoustic imaging to differentiate atherosclerotic plaques. *Opt Express* 2008; 16:3362–3367
57. Wang X, Ku G, Wegiel MA, Bornhop DJ, Stoica G, Wang LV. Noninvasive photoacoustic angiography of animal brains in vivo with near-infrared light and an optical contrast agent. *Opt Lett* 2004; 29:730–732
58. De la Zerda A, Zavaleta C, Keren S, et al. Carbon nanotubes as photoacoustic molecular imaging agents in living mice. *Nat Nanotechnol* 2008; 3:557–562
59. Eghtedari M, Oraevsky A, Copland JA, Kotov NA, Conjusteau A, Motamedi M. High sensitivity of in vivo detection of gold nanorods using a laser optoacoustic imaging system. *Nano Lett* 2007; 7:1914–1918
60. Taruttis A, Herzog E, Razansky D, Ntziachristos V. Real-time imaging of cardiovascular dynamics and circulating gold nanorods with multispectral optoacoustic tomography. *Opt Express* 2010; 18:19,592–19,602
61. Mallidi S, Larson T, Tam J, et al. Multiwavelength photoacoustic imaging and plasmon resonance coupling of gold nanoparticles for selective detection of cancer. *Nano Lett* 2009; 9:2825–2831
62. Ermilov SA, Khamapirad T, Conjusteau A, et al. Laser optoacoustic imaging system for detection of breast cancer. *J Biomed Opt* 2009; 14:024007
63. Manohar S, Vaartjes SE, van Hespen JCG, et al. Initial results of in vivo non-invasive cancer imaging in the human breast using near-infrared photoacoustics. *Opt Express* 2007; 15:12,277–12,285
64. Kim C, Erpelding TN, Jankovic L, Wang LV. Performance benchmarks of an array-based hand-held photoacoustic probe adapted from a clinical ultrasound system for non-invasive sentinel lymph node imaging. *Philos Transact A Math Phys Eng Sci* 2011; 369:4644–4650
65. Fronheiser MP, Ermilov SA, Brecht HP, et al. Real-time optoacoustic monitoring and three-dimensional mapping of a human arm vasculature. *J Biomed Opt* 2010; 15:021305
66. Favazza CP, Jassim O, Cornelius LA, Wang LV. In vivo photoacoustic microscopy of human cutaneous microvasculature and a nevus. *J Biomed Opt* 2011; 16:016015
67. Bézière N, Ntziachristos V. Optoacoustic imaging: an emerging modality for the gastrointestinal tract. *Gastroenterology* 2011; 141:1979–1985
68. Stummer W, Novotny A, Stepp H, Goetz C, Bise K, Reulen HJ. Fluorescence-guided resection of glioblastoma multiforme by using 5-aminolevulinic acid-induced porphyrins: a prospective study in 52 consecutive patients. *J Neurosurg* 2000; 93:1003–1013
69. Yao J, Maslov KI, Zhang Y, Xia Y, Wang LV. Label-free oxygen-metabolic photoacoustic microscopy in vivo. *J Biomed Opt* 2011; 16:076003

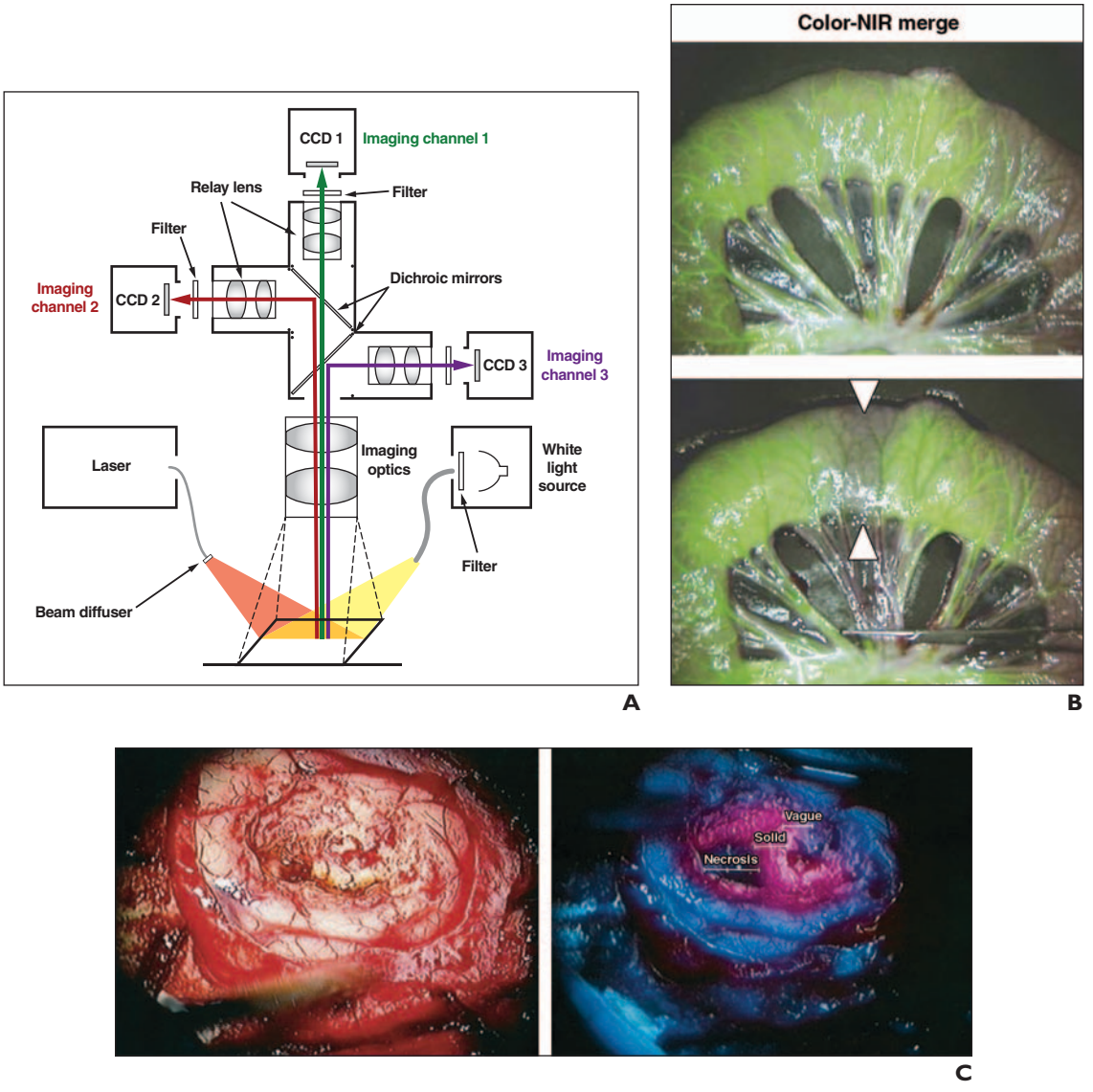


**Fig. 1**—Fluorescence-guided surgery.
**A,** Diagram shows multispectral camera system that is used for fluorescence-guided surgery. CCD = charge-coupled device. (Reprinted with permission from Macmillan Publishers Ltd.: *Nature Medicine* [24], copyright 2011)
**B,** Photographic images of small bowel from pig. Top image was obtained before clamp was placed and bottom image was obtained after clamp was placed. Green overlay shows near-infrared fluorescence signal from indocyanine green. Arrowheads indicate ischemic region. (Reprinted with permission from John Wiley and Sons [13]: Matsui A, Winer JH, Laurence RG, Frangioni JV. Predicting the Survival of Experimental Ischaemic Small Bowel Using Intraoperative Near-Infrared Fluorescence Angiography. *Br J Surg* 2011; 98:1725–1734)
**C,** Intraoperative photographs of brain tumor cavity after administration of 5-aminolevulinic acid under normal white light (*left*) and under violet-blue illumination (*right*). (Reprinted with permission from the American Association of Neurological Surgeons [68]: Stummer W, Novotny A, Stepp H, Goetz C, Bise K, Reulen HJ. Fluorescence-guided resection of glioblastoma multiforme by using 5-aminolevulinic acid-induced porphyrins: a prospective study in 52 consecutive patients. *J Neurosurg* 2000; 93:1003–1013)

**(Fig. 1 continues on next page)**

**Fig. 1 (continued)**—Fluorescence-guided surgery.
**D,** Color photographic image (*left*) and corresponding fluorescence image (*right*) after injection of tumor-targeting folate–fluorescein isothiocyanate. (Reprinted with permission from Macmillan Publishers Ltd.: *Nature Medicine* [24], copyright 2011)
**E,** Graph shows scoring based on three different pairs of color and fluorescence images by five independent surgeons asked to count number of visible tumor spots. (Reprinted with permission from Macmillan Publishers Ltd.: *Nature Medicine* [24], copyright 2011)

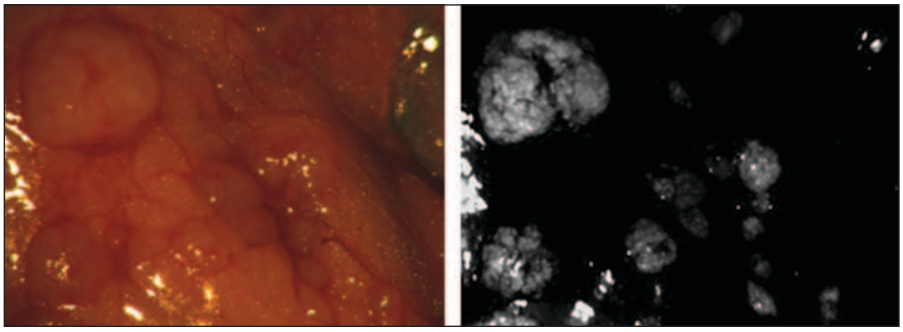

D

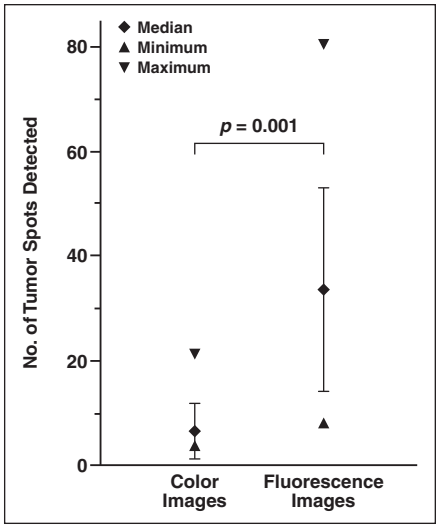


E

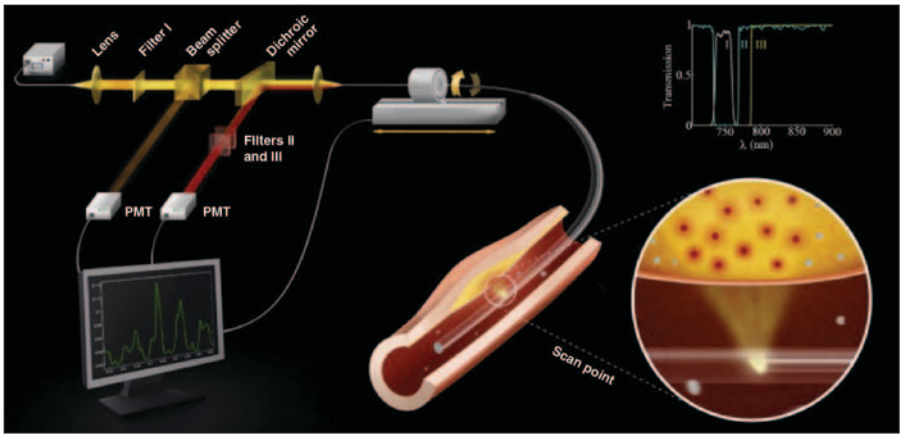


A


B

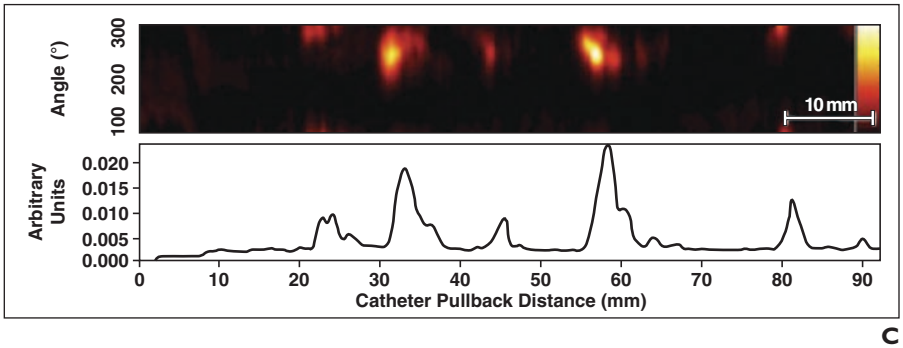


C

**Fig. 2**—Intravascular fluorescence imaging.
**A,** Illustration shows fluorescence catheter system. PMT = photomultiplier tube. (Reprinted from the *Journal of the American College of Cardiology*, Vol. 57/edition 25. Jaffer FA, Calfon MA, Rosenthal A, et al. Two-Dimensional Intravascular Near-Infrared Fluorescence Molecular Imaging of Inflammation in Atherosclerosis and Stent-Induced Vascular Injury. Pages 2516–2526, Copyright 2011, with permission from Elsevier)
**B,** Imaging of inflamed atheroma in rabbit. Longitudinal intravascular ultrasound image of abdominal aortoiliac arteries shows plaques labeled $P_1$ and $P_2$ (*arrowheads*). (Reprinted from the *Journal of the American College of Cardiology*, Vol. 57/edition 25. Jaffer FA, Calfon MA, Rosenthal A, et al. Two-Dimensional Intravascular Near-Infrared Fluorescence Molecular Imaging of Inflammation in Atherosclerosis and Stent-Induced Vascular Injury. Pages 2516–2526, Copyright 2011, with permission from Elsevier)
**C,** Imaging of inflamed atheroma in rabbit (same as that shown in **B**). Near-infrared (NIR) fluorescence image (*top*) of catheter pullback aligned with intravascular ultrasound image shows signal from protease-activated agent originating in plaques. Signal intensity shown in top image is plotted in one-dimensional graph (*bottom*). (Reprinted from the *Journal of the American College of Cardiology*, Vol. 57/edition 25. Jaffer FA, Calfon MA, Rosenthal A, et al. Two-Dimensional Intravascular Near-Infrared Fluorescence Molecular Imaging of Inflammation in Atherosclerosis and Stent-Induced Vascular Injury. Pages 2516–2526, Copyright 2011, with permission from Elsevier)

**(Fig. 2 continues on next page)**

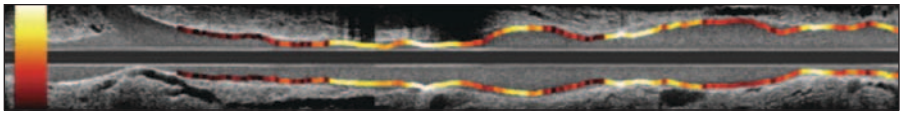

D

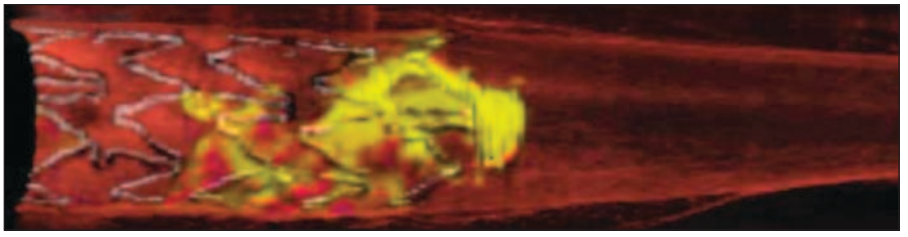

E

**Fig. 2 (continued)**—Intravascular fluorescence imaging.
**D,** Imaging of inflamed atheroma in rabbit model (same as that shown in **B** and **C**). Longitudinal superimposed intravascular ultrasound image and NIR fluorescence image are shown. Yellow and white represent highest NIR fluorescence intensity. (Reprinted from the *Journal of the American College of Cardiology*, Vol. 57/edition 25. Jaffer FA, Calfon MA, Rosenthal A, et al. Two-Dimensional Intravascular Near-Infrared Fluorescence Molecular Imaging of Inflammation in Atherosclerosis and Stent-Induced Vascular Injury. Pages 2516–2526, Copyright 2011, with permission from Elsevier)
**E,** Stented right iliac artery in rabbit. Image is example of merge of optical frequency domain imaging, which allows microstructural visualization of stent, and NIR fluorescence signal originating from fluorescent fibrin with which stent was coated. Red = artery wall, white = stent, yellow = NIR fluorescence fibrin. Scale: 500 μm. (Reprinted with permission from MacMillan Publishers Ltd.: *Nature Medicine* [29], copyright 2011)

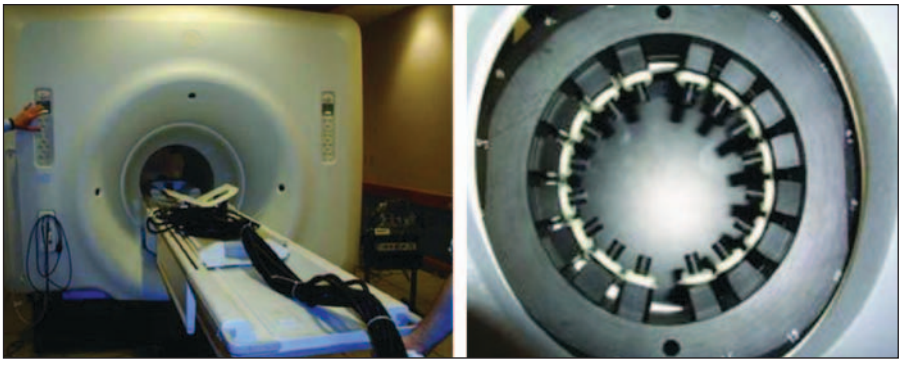

A

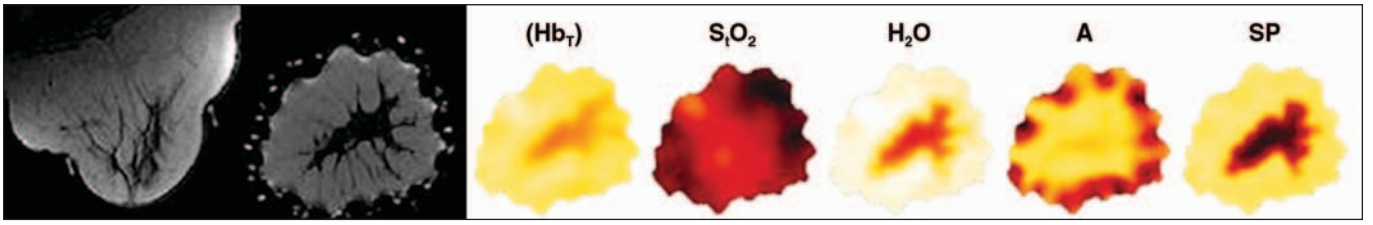


B

**Fig. 3**—Multispectral diffuse optical tomography for breast imaging.
**A,** Left photograph shows clinical MRI unit combined with optical fiber–based diffuse optical tomographic breast imager. Right photograph shows fiber orientation around breast.
**B,** Representative results from healthy breast. Images are shown from left to right as follows: axial and coronal T1-weighted MR images and diffuse optical tomographic images of total hemoglobin concentration map ($Hb_T$), hemoglobin oxygen saturation ($S_tO_2$), water fraction ($H_2O$), optical scattering amplitude (A), and scattering power (SP). (Reprinted with permission from [32]; copyright 2006 National Academy of Sciences, U.S.A.)

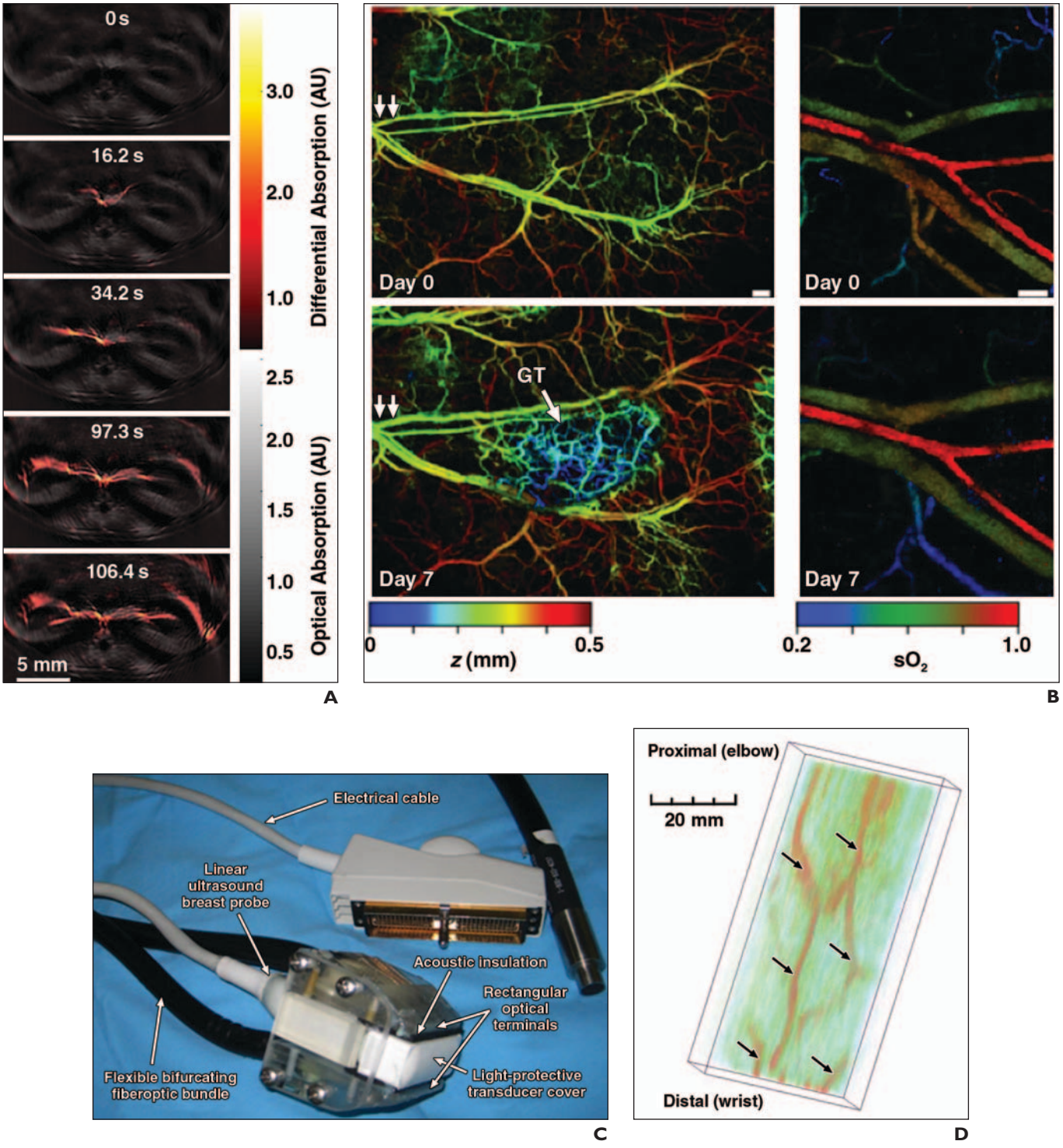


**Fig. 4**—Optoacoustic imaging.
**A,** Real-time optoacoustic tomography sequence show indocyanine green via differential absorption as it enters kidneys of mouse.
**B,** Multispectral optoacoustic microscopy images (*left*) show microvasculature in region of early stage glioblastoma (GT) mouse model. *z* = catheter pullback distance. Functional images (*right*) show hemoglobin oxygenation saturation ($sO_2$) in artery-vein pair that supports tumor, indicated by arrows in images on left. (Reprinted with permission from [69]: Yao J, Maslov KI, Zhang Y, Xia Y, Wang LV. Label-Free Oxygen-Metabolic Photoacoustic Microscopy In Vivo. *J Biomed Opt* 2011; 16:076003)
**C,** Photograph shows typical handheld optoacoustic imaging system for experimental clinical use. Main components of system are ultrasound transducer array and optical fiber bundle for delivery of excitation light.
**D,** Map of blood vessels (arrows) in human arm that was produced by handheld optoacoustic imaging system. (Reprinted with permission from [65]: Fronheiser MP, Ermilov SA, Brecht HP, et al. Real-time optoacoustic monitoring and three-dimensional mapping of a human arm vasculature. *J Biomed Opt* 2010; 15:021305)